Simulation, parameters and performance of the three-phase phase-controlled full-wave rectifier with RL load

Danissa Sandykbayeva
Robotics and Mechatronics
Nazarbayev University
Nur-Sultan, Kazakhstan
danissa.sandykbayeva@nu.edu.kz

***Abstract*—Full-wave rectifiers share the same main purpose with the half-wave rectifiers: to produce a current or voltage that is purely DC, or the one that has specified DC component. However, full-wave rectifiers produce smaller ripple and have a zero average AC source current. This conference paper discusses estimations of the main parameters of the three-phase full-wave rectifiers with RL load that would make output characteristics meet the given requirements. Results of this paper are also simulated in the Simulink software.**

***Index Terms*—full-wave rectifiers, phase-controlled rectifiers, three-phase rectifiers,**

I. Introduction

Phase-controlled rectifiers, and silicon-controlled rectifiers(SCR) are widely used in the fields of electronics were management of average-to-high voltage or power parameters is demanded. Application fields include, and are not limited to motor control and design, power transmission and regulation systems, etc. In addition, three-phase rectifiers are generally used for DC voltage production when working with large power and loads. The main purpose of this paper is to examine and estimate main parameters for the controlled three-phase rectifier circuit with RL load that would best approximate provided requirements. Additionally those parameters have to be tested on practice using the simulation software, which includes designing the appropriate circuitry in Simulink and final tuning of the parameters.

II. Methods

A. Requirements of the system

For the purpose of this paper the following requirements had to be met by the final circuit design:

- V_m (phase voltage) = 300 V
- f = 60 Hz
- P_{load} = 100 kW
- V_o = 300 V
- ΔI = 2%

B. Theory and calculations

1) Delay angle: The main parameter that affects the output voltage waveform and its DC component in controlled rectifiers is a delay angle - α. Three-phase fully-controlled rectifiers uses six thyristors/SCR assembled in a form of a full-wave bridge configuration. Thyristors are triggered at appropriate times specified by the phase delay and sample time. The delay angle represents an interval between two time instances: when SCR becomes forward-biased and when the gate signal is applied. The general configuration for the controlled three-phase rectifier is shown on the Fig. 1

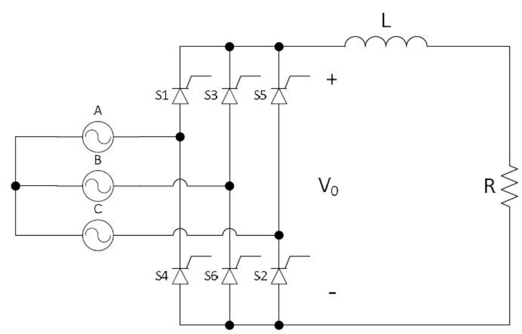

Fig. 1. Controlled three-phase rectifier

The average output voltage is determined by the following equation:

$$V_o = \frac{1}{\pi/3} \int_{2\pi/3}^{\pi/3} V_{m,L-L} sin(wt) d(wt)$$
$$= \frac{3V_{m,L-L}}{\pi} cos\ \alpha$$

Considering that the given requirements have specified V_m we substitute it with the line-to-line voltage according to the formula of $V_m = \sqrt{3} V_{m,L-L}$ resulting in:

$$V_o = \frac{3\sqrt{3}V_m}{\pi} cos\ \alpha$$

Therefore, the delay angle corresponding to initial requirements would be:

$$\alpha = cos^{-1}(\frac{V_o \pi}{3\sqrt{3}V_m}) \approx 52.80° \tag{1}$$

Furthermore, output voltage wave-forms should follow the shape similar to the one illustrated on Fig 2.

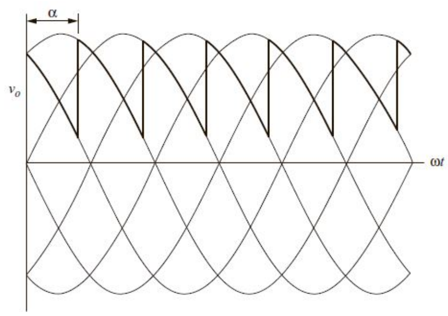

Fig. 2. Outputvoltage of a controlled three-phase rectifier for $\alpha = 45°$

Two remaining parameters of the circuit are resistance (R) and inductance (L).

2) Resistance and output current: Firstly, resistance directly affects our requirement of the power of the load P_{load} = 100 kW, since $P_{load} = I_{rms}^2 R$. Since full-wave controlled rectifiers provide a relatively stable output current with minimal ripple we could make an approximation of I_{rms} being equal to I_o. This leads us to the first equation:

$$P_{load} = I_o^2 R = 100\ kW \tag{2}$$

Furthermore, since we have two unknown variables in this case we take into account the output requirements for the voltage. Considering that output voltage depends on the resistance only we have:

$$V_o = I_o R = 300\ V \tag{3}$$

Resistance now can be calculated along with the output dc current value using the system of (2) and (3)

$$\begin{cases} I_o^2 R = 10^5\ W \\ I_o R = 300\ V \end{cases} \tag{4}$$

Solving this system we get the values for $R = 0.9\ \Omega$ and $I_o \approx 333.3\ A$.

3) Inductance: Last parameter that defines the discussed system's performance is inductance. While resistance affects the power on load, inductance is responsible for control of the current, it's ripple and reactive power. The specification given for the ripple $\Delta I = 2\%$ which is the variation in the load current generated due to the AC terms of I_{rms} described by the Fourier series in (5)

$$I_n = \frac{V_n}{Z_n}$$
$$Z_n = \sqrt{R^2 + (nwL)^2} \tag{5}$$

Moreover, since with increasing number of harmonics $n = [1, 6, 12, ...]$ V_n is decreasing significantly and Z_n is increasing, the ripple or the change in the load current could be described with it's difference from the first AC term (n=6, for the first AC term). To estimate V_6 we use the graph of the normalized output voltage harmonics as a function of a delay angle given on the Fig. 3

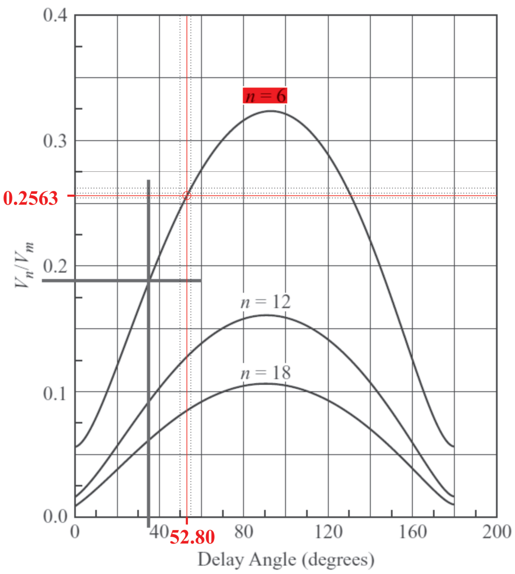

Fig. 3. Normalized output voltage harmonics as a function of delay angle for three-phase rectifier

From the earlier estimated delay angle $\alpha = 52.80°$, $V_6/V_{m,L-L}$ at n = 6 is estimated to be 0.2563. Therefore, $V_6 = 0.2563 V_{m,L-L} = 0.2563\sqrt{3} V_m$. Moreover, considering that $\Delta I = 2\%$ corresponds to peak-to-peak variation, the zero-to-peak amplitude for the load current at n-6 would be $\frac{0.02}{2} I_o$. The load impedance required then would be:

$$Z_6 = \frac{V_6}{I_6} = \frac{0.2563\sqrt{3} V_m}{0.01 I_o}$$
$$= 39.99\ \Omega \tag{6}$$

Now considering (5) and the estimated value of the resistance $R = 0.9\ \Omega$ we obtain the equation for the inductance required in order to meet the load current variance requirements:

$$w = 2\pi f \approx 377\ rad/s$$

$$0.9^2 + (6 \cdot 377L)^2 = 39.99^2$$

$$0.81 + 36 \cdot 377^2 L^2 = 1599.20$$

$$L = 0.0177\ H = 17.67\ mH \tag{7}$$

C. Simulation

All of the calculated parameters for RL load and the delay angle are tested by designing a firing circuit for the topology given on Fig. 1. All simulations are made using Simulink software (Simscape library and Simulink general libraries)

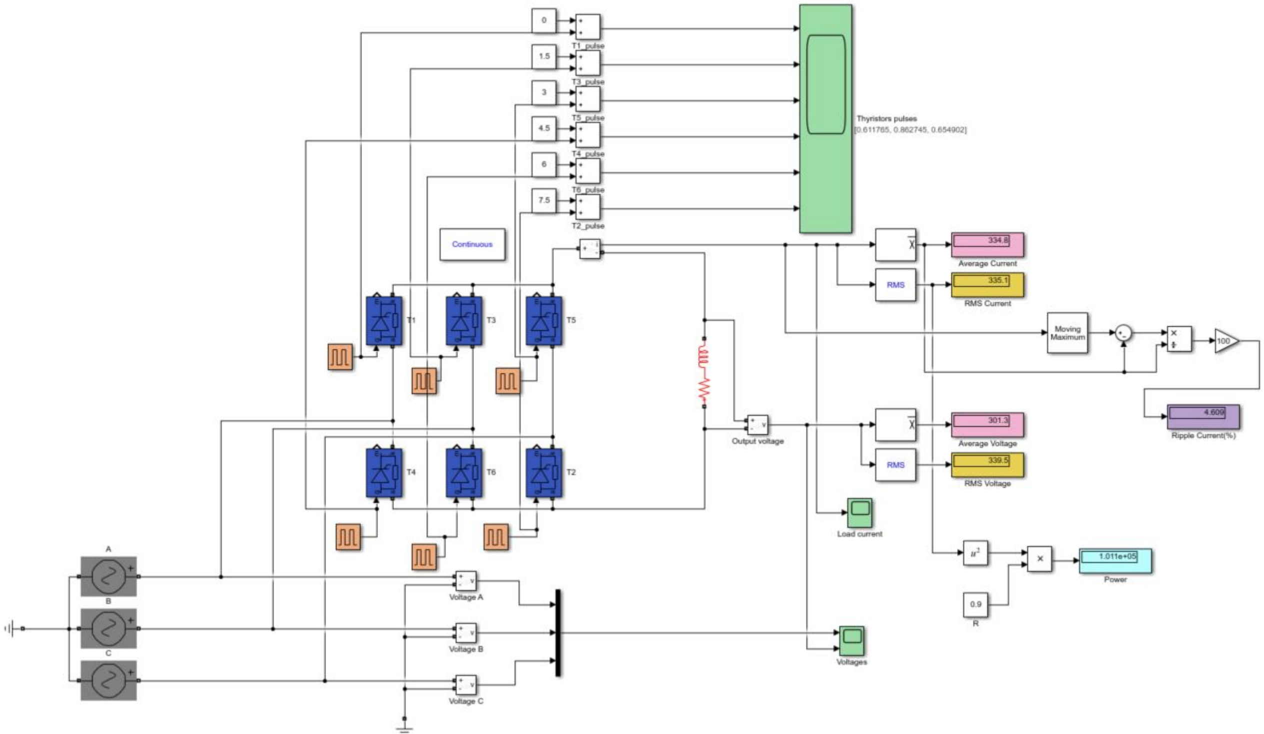

Fig. 4. Three-phase controlled full-wave rectifier, Simulink

1) Defining three-phase AC supply: For the three-phase controlled rectifier all three voltage supplies share the same peak-to-peak voltage, but have the phase difference of 120°. "AC Voltage Source" blocks from the Simscape library (Fig. 4) are used for this purpose with the incoming parameters of

- Peak amplitude (V) = 300
- Phase (deg) = 0 (for V_A),120 (for V_B),240/-120 (for V_C)
- Frequency (Hz) = 60

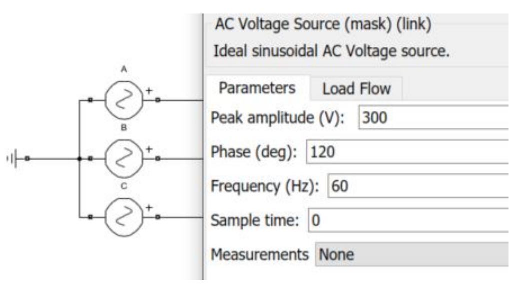

Fig. 5. 'AC Voltage source' Simulink block' configurations

2) Thyristors pulse-firing scheme: Three-phase controlled rectifier also consists of six thyristors that are triggered consecutively. Each pair of thyristors is triggered at an interval of $\frac{\pi}{3}$ (pairs: 6-1,1-2,2-3,3-4,4-5,5-6), while each thyristor gets triggered individually every $\frac{2\pi}{3}$. This means that T_1 is triggered at $(30° + \alpha)$, T_3 is triggered at $(30° + \alpha + 120°)$, etc.

In order to simulate such behaviour in Simulink two kinds of Simscape blocks are used: 6 "Thyristor" blocks and 6 "Pulse Generator" blocks correspondingly. The only parameters that should be essentially changed are for the pulse generators:

- Period (secs): 1/60
- Pulse width (% of period): 100/3
- Phase delay (secs): $\frac{\alpha + n \cdot 30°}{360° \cdot 60}$, where n depends on the thyristor

The final topology for thyristors connection scheme is shown on the Fig. 4 The rest of the blocks used in the circuit are RL branch, blocks for measuring current and voltage, calculating the load power and current variance. The final Simulink topology is illustrated on the Fig. 6. For the convenience, different types of blocks have designated colors, which are distributed as the following:

- Blue - Thyristor
- Orange - Pulse generator
- Gray - AC source
- Green - Scopes for the measurement graph
- Pink - Average/mean measurement
- Yellow - RMS measurement
- Violet - Variance in the current, calculated as $= \frac{I_{max} - I_{avg}}{I_{avg}} \cdot 100\%$
- Cyan - Load power, calculated as $= I_{rms}^2 R$
- Red - RL branch

3) Measurements: For load current and voltage both RMS and average values are estimated from the measured signals and shown on corresponding displays. Math-operational

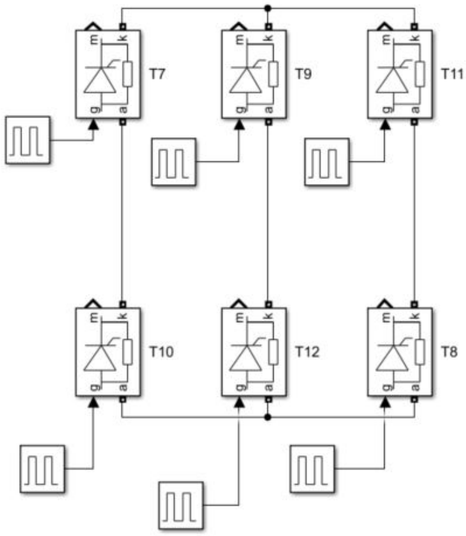

Fig. 6. 6 Thyristors with Pulse Generators

blocks and 'Moving maximum' are used in order to measure load power and load current variance.

4) Scopes: The largest scope provides the picture of pulses generated for 6 thyristors in sequence. Constants of $1.5 \cdot n$ are sequentially added to each pulse in order to plot all of the pulses on one scope, avoiding overlapping. 'Voltages' scope provides the overview of all incoming voltages from AC sources and the voltage generated across the load. 'Load current' scope simply shows the current across the load.

5) RL branch: For resistance and inductance, in 'RL branch' block, values calculated in (4) and (7) are used:

$$R = 0.9\ \Omega;\ L = 0.0177\ H$$

III. Simulation Results and Discussion

First of all we need to check if the pulses generated for thyristors actually follow the prescribed pattern. The of the 'Thyristor pulses' scope is presented on the Fig. 6 The pulses

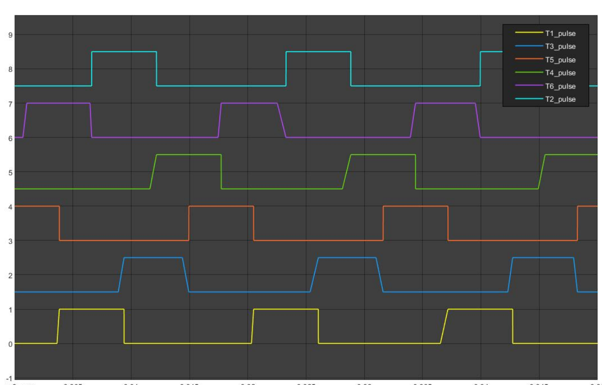

Fig. 7. Generated signals for 6 Thyristors system

are indeed following the designed firing scheme described in previous sections of "Methods"

Next the voltage wave-forms are verified, which are presented on Fig. 6. Voltage wave-forms again follow the general shape illustrated by the Fig. 2. When in comes to the values of V_{rms} and V_{avg} both of them could be seen (Fig. 7) to come relatively close to the initial requirement of 300V Since

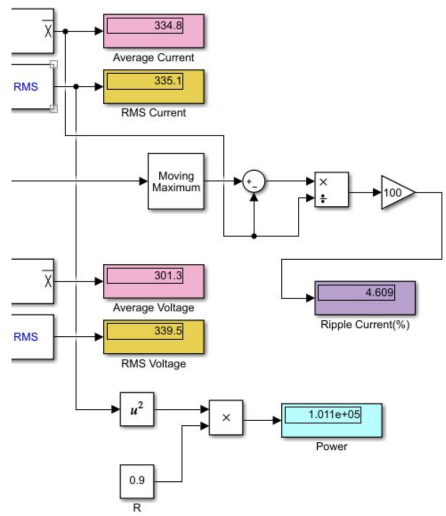

Fig. 8. Numerical results of the simulation

we are mostly interested in the average output voltage of the circuit, we could say that the voltage requirements we met since the difference between the obtained and required voltage of $301.3 - 300$ constitutes only 0.43% of 300V The last graph generated by the scopes of the circuit is load current on Fig. 8 There two requirements that were supposed to be

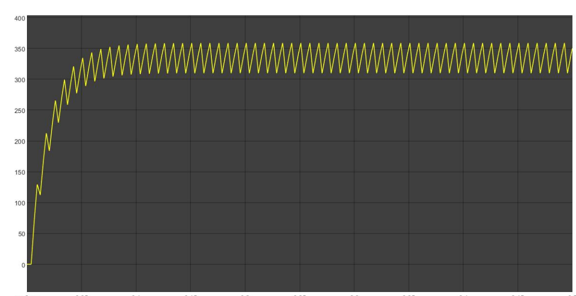

Fig. 9. Load current of the simulation

checked: $P_{load} = 100\ kW$ and $\Delta I_o \approx 2\%$. Firstly the power requirement according to the output results on Fig.7 have been met, since the obtained power load value of $1.011 \cdot 10^5\ W$ is bigger than the required result of $10^5\ W$ only by 1.1%. The second condition of the variance in current however, is pretty different from the estimated/required value of 2%, since from the Fig. 7 $\Delta I_{obtained} = 4.609\%$ which is little than twice higher than the original value. This error might generated due to the various approximations made while estimating inductance value, such as the harmonics approximation, etc. Moreover, we could try now to just tune the inductance value to make variance in the load current meet the requirements, and turns out that for the inductance value of $L = 0.038\ H$ the power generated on the load remains the same, but the current ripple becomes $\Delta I_o = 2.074\%$ which could now be said to be relatively close to the original requirement of 2%. This change in inductance value also implies that with higher inductance, a current ripple becomes smaller.

IV. Conclusion

The final estimated parameters:

$$R = 0.9\ \Omega;\ I_o = 333.3\ A$$

$$L = 0.038\ H;\ \alpha = 52.8^\circ$$

All of the initial requirements have been met, even though obtaining proper current variance required some additional tuning the to the values that differ from our calculated ones. On the other hand the remaining requirements of load power, average output voltage followed the behaviour predicted in the "Calculations" section of the paper.

References

[1] Hart, Daniel W "Power Electronics," The McGraw-Hill Companies. New York, 10th Edition, pp. 149–156, 2011.